APP Template V1.70 Article id: sust519231 Typesetter: MPS Date received by MPS: 25/08/2015 PE: MAC003439 CE: LE:

OPEN ACCESS
IOP Publishing
Superconductor Science and Technology
Supercond. Sci. Technol. **00** (2015) 000000 (12pp)

Q1

Application potential of Fe-based superconductors

Ilaria Pallecchi[1], Michael Eisterer[2], Andrea Malagoli[1] and Marina Putti[1]

Q2 [1] CNR-SPIN and University of Genoa, c/o dipartimento di Fisica, via Dodecaneso 33, 16146 Genova, Italy
[2] Atominstitut, TU Wien, A-1020 Vienna, Austria

Received 15 June 2015, revised 14 August 2015
Accepted for publication 18 August 2015
Published DD MM 2015

Abstract

In this paper we report basic properties of iron-based superconductors and review the latest achievements in the fabrication of conductors based on these materials. We compare state-of-the-art results with performances obtained with low-T_c and high-T_c technical superconductors, evidencing in particular the most significant differences with respect to high-T_c cuprate coated conductors. Although the optimization of preparation procedures is yet to be established, a potential range of applications for iron-based superconductors in the high field low temperature regime can be envisaged, where they may become competitors to RE-123 coated conductors.

Keywords: iron-based superconductors, powder-in-tube, application potential

SQ1 (Some figures may appear in colour only in the online journal)

1. Introduction

Soon after the discovery of superconductivity in iron-based superconductors (FeSCs) [1], their very high upper critical fields, low anisotropy and large J_c values, which are only weakly reduced by magnetic fields at low temperatures, suggested considerable potential in large scale applications, particularly at low temperature and high fields [2, 3]. Among the different families, the 122 compounds with a chemical composition of AFe_2As_2 (A = alkaline earth metal) appear to be the most promising, as they are the least anisotropic, have a fairly large T_c of up to 38 K, close to that of MgB_2, and exhibit large critical current densities. However, 122 compounds contain toxic As and reactive alkaline earth metals, which may be a problem for large scale fabrication processes. In this respect, 1111 compounds with the chemical composition LnFeAsO (Ln = Lanthanides) present problems as well, as they contain As as well as volatile F and O, whose stoichiometry is hardly controlled. 11 compounds with the chemical composition FeCh (Ch = chalcogen ion) have a lower T_c of up to 16 K, but they contain no toxic or volatile elements. It is worth mentioning that new iron-based superconducting families and compounds are regularly discovered, such as for example the 112 compounds (Ca,*RE*)$FeAs_2$ (*RE* = rare earth such as La,Ce,Pr,Sm,Eu,Gd) with T_c up to ~40 K [4], the 42 214 compounds $RE_4Fe_2As_2Te_{1-x}O_4$ with T_c up to ~45 K for *RE* = Gd [5], the 21 311 compounds Sr_2MO_3FeAs (M = Sc, V, Cr) with $T_c \sim 37$ K [6] and [(Li, Fe)OH]FeSe with T_c up to ~40 K [7].

Thanks to a small coherence length of a few nanometers [2], FeSCs are particularly sensitive to the inclusion of nanoparticles and to local variation of stoichiometry as pinning centers to enhance the critical current density. For example, the pinning force in 122 films was enhanced above that of optimized Nb_3Sn at 4.2 K by the introduction of self-assembled $BaFeO_2$ nanorods [8], while similar effects were obtained due to local variations of stoichiometry in 11 films [9, 10]. Critical current J_c values exceeding 10^5 A cm^{-2} were measured in FeSCs films of 11, 122 and 1111 families up to very large magnetic fields either parallel or perpendicular to the Fe planes. In particular a J_c above 10^5 A cm^{-2} was achieved up to 18 T in P-doped $BaFe_2As_2$ films [11], up to 30 T in $FeSe_{0.5}Te_{0.5}$ films [9] and up to 45 T in SmFeAs(O,F) films [12]. Record values of self-field critical current densities up to 6 MA cm^{-2} at 4.2 K were measured in 122 films [11, 13] and up to 20 MA cm^{-2} at 4.2 K in zero field in 1111 single crystals irradiated with heavy ions [14]. Furthermore, nanometer scale disorder proved to suppress T_c only very weakly [8, 14], suggesting that yet further improvements of flux pinning are achievable. In the following, the basic properties of FeSCs and the most important achievements in

Table 1. Relevant iron-based compounds and technical superconductors. The highest T_c found in each respective family is given. T^{op} refers to a typical or expected operation temperature.

Compound	Code	max. T_c (K)	T^{op} (K)	
$LnFeAsO_{1-x}F_x$	1111	58 [15]	$\leqslant$40 (?)	Ln = Sm, Nd, La, Pr,….
$BaFe_2As_2$[a]	122	38 [18]	$\leqslant$25	K, Co, or P doping
$FeSe_{1-x}Te_x$	11	16 [19]	$\leqslant$4.2	
Nb-Ti	—	10	$\leqslant$4.2	
Nb_3Sn	—	18	$\leqslant$4.2	
MgB_2	—	39	$\leqslant$25	
RE-$Ba_2Cu_3O_{7-x}$	RE-123	95	$\leqslant$77	RE = Y, Gd, Sm, Nd, Yb,…
$Bi_2Sr_2CaCu_2O_{8-x}$	Bi-2212	85	$\leqslant$20	
$Bi_2Sr_2Ca_2Cu_3O_{10-x}$	Bi-2223	110	$\leqslant$77	

[a] Ba can be replaced by Sr or Ca.

the development of practical conductors are reviewed with respect to established results on other superconductors. An assessment of the application potential of FeSCs is attempted, based on properties and promising results measured on short specimens. On the other hand, the issue of upscaling preparation procedures must certainly be faced in the future, but iron-based wire technology is currently far less mature than other technologies such as that of $YBa_2Cu_3O_7$ coated conductors.

2. Basic properties

The basic properties set the final performance limit of a superconducting material in terms of temperature, field and critical current. These properties of the most relevant FeSCs will be reviewed in this section and compared to those of established technical superconductors.

2.1. Transition temperature

The highest transition temperature of all FeSCs was found in the 1111 compound $T_c \sim 58$ K [15] (see table 1), which places this compound between the cuprates and MgB_2. The transition temperature T_c is defined as the temperature up to which superconductivity persists. However, applications are restricted to lower temperatures, since superconductivity becomes very weak close to T_c. As a rule of thumb, the operation temperature T^{op} should be about half of T_c or lower in applications requiring high currents and/or fields. However, strong thermal fluctuations of the vortex lattice reduce the critical currents significantly in highly anisotropic materials, restricting appropriate operation conditions to much lower temperatures. $(Bi,Pb)_2Sr_2Ca_1Cu_2O_x$ (Bi-2212) is an extreme example that provides useful current densities only at temperatures below about 20 K, despite its high transition temperature of 85 K. The anticipated maximum operation temperatures of the FeSCs are given in table 1 together with values for other superconducting compounds. Note that the higher the required magnetic field, the lower the operation temperature must be. Since the 1111 compounds are the most anisotropic of all considered FeSCs, the estimated value for the maximum T^{op} has to be confirmed when long length conductors become available, and may be restricted to low magnetic fields. In any case, all FeSCs discovered so far are obviously no alternative to $REBa_2Cu_3O_7$ (RE-123) coated conductors or $(Bi,Pb)_2Sr_2Ca_2Cu_3O_x$ (Bi-2223) tapes at high temperature (>50 K), in particular for use with nitrogen as the coolant.

K-doped $BaFe_2As_2$ (Ba-122) has a transition temperature of around 38 K, nearly the same as MgB_2. From this viewpoint, the two materials are direct competitors for applications at intermediate temperatures, which do not rely on liquid helium as a coolant. P- or Co-doped Ba-122 have lower T_cs of about 30 K and 24 K, respectively, which makes helium free operation questionable. The 11 compounds have the lowest T_cs, even below that of the readily available Nb_3Sn, thus helium cooling is the only option.

Although many new iron-based compounds have been discovered, T_c has not significantly increased over the past few years. However, superconducting-like energy gaps between 55 K and 75 K were found by angle resolved photoemission spectroscopy (ARPES) inspections in a single layer of FeSe on top of doped $SrTiO_3$ [16], possibly resulting from a charge transfer between the superconducting layer and the substrate. Unambiguous evidence of a transition to zero resistivity and diamagnetic behavior is yet to be widely established in this system at such high temperatures, although a highly non-linear behavior in the I–V curves up to about 100 K was derived from a particular *in situ* four-point probe technique [17], which exactly fits the expected behavior of a superconductor. The temperature and field dependencies of the derived J_c and resistivity are also consistent with superconductivity. These results fuel the hope that higher T_cs are achievable in iron-based compounds with as yet unknown interlayers.

2.2. Upper critical field

The upper critical field B_{c2} limits the field which can be generated using the respective superconductor; maximally about $0.75 \cdot B_{c2}$ can be effectively achieved. Since superconducting wires are used nowadays nearly exclusively for magnets, B_{c2} is certainly a key parameter for applications and restricts available magnets based on conventional (niobium-based) technology to fields below 25 T. Novel conductors for

the next generation of NMR, accelerator, research, and fusion magnets are urgently needed. While MgB_2 is unsuitable for high field magnets, cuprates and FeSCs have upper critical fields in the 50–100 T range (and even greater) at 4.2 K, thus not imposing any realistic limitations for high field magnets operating at low temperatures. On the other hand, B_{c2} decreases with temperature and converges to zero at T_c, thus a high $B_{c2}(0\,K)$ is, besides a high-T_c, a prerequisite for cryo-cooled magnets operating at intermediate fields (e.g. medical MRI magnets). In this respect, FeSCs are clearly favorable compared to MgB_2, which is already applied in low field MRI systems.

An important point to mention is the low anisotropy of the upper critical field $B_{c2}^{(ab)}/B_{c2}^{(c)}$ in the FeSCs, which makes flux pinning more efficient than in the highly anisotropic cuprates by reducing flux cutting effects and thermal fluctuations. In particular, the 11 and 122 compounds are nearly isotropic at low temperatures [2, 20]. Although the anisotropy increases with temperature in these compounds, reaching values up to about 3 close to T_c, it remains well below that of *RE*-123 coated conductors (≈5) and Bi-tapes (>20), also at high temperatures.

2.3. Critical current densities

The critical current density in a superconducting wire is either limited by flux pinning or granularity (see section 2.4). Flux pinning is an extrinsic property, which can be tuned by generating a suitable defect structure. The maximally achievable loss free currents are, however, not independent from the basic material parameters, since J_c amounts to maximally 10–20% of the depairing current density, J_d, in optimized materials. J_d is a material property and can be estimated from the coherence length ξ and London penetration depth λ as $J_d \sim \phi_0/3\sqrt{3}\,\pi\mu_0\lambda^2\xi$ (ϕ_0 is the flux quantum and μ_0 the vacuum permeability). J_d values in the zero temperature limit can reach up to $3 \cdot 10^8\,A\,cm^{-2}$ in cuprates [21], about $1.8 \cdot 10^8\,A\,cm^{-2}$ in Nb_3Sn (assuming $\xi = 3.6\,nm$ and $\lambda = 124\,nm$) [22] and $2 \cdot 10^8\,A\,cm^{-2}$ in MgB_2 [23]. It turns out similar in $SmFeAsO_{1-x}F_x$ and K-doped Ba-122 (about $1.7 \cdot 10^8\,A\,cm^{-2}$), but smaller in the P- and Co-doped 122 system (≈5 and $9 \cdot 10^7\,A\,cm^{-2}$, respectively) and only around $2 \cdot 10^7\,A\,cm^{-2}$ in the 11 system [20]. Thus at least some compounds can compete with the high values in cuprates, MgB_2, and Nb_3Sn.

Efficient pinning can be realized comparatively easily in the iron-based materials, as demonstrated by irradiation experiments [14, 24], by the successful introduction of nanoparticles [13] or nanorods [8, 25], by the effect of local variation of stoichiometry [9, 10]. Moreover, irradiation with Au ions [26] and neutrons [27] and introduction of artificial *ab* plane pins [28] emphasized that the introduction of pinning defects does not affect T_c appreciably. This indicates that FeSCs tolerate a higher density of defects without a significant decrease in T_c than cuprates, which makes them ideal candidates for high field applications, since the number of pinning centres is of crucial importance at high fields.

Another key property of FeSCs relevant for applications is the small anisotropy of J_c with respect to the crystal axis. Direct transport J_c measurements in the two main crystallographic directions $J_c^{(ab)}$ and $J_c^{(c)}$ were carried out on Sm-1111 single crystals with patterned micro-bridges [29] and on $Ba(Fe_{1-x}Co_x)_2As_2$ single crystals using the Montgomery technique [30]. The obtained $J_c^{(ab)}/J_c^{(c)}$ ratios were 2.5 and 1.5 respectively, much lower than the values of up to 10–50 found in the cuprates [31].

2.4. Grain coupling

All high-T_c superconductors are prone to magnetic granularity, which limits the macroscopic currents. While secondary phases residing at the grain boundaries and voids reduce the cross section over which the current effectively flows in MgB_2, high angle grain boundaries intrinsically limit the currents in untextured polycrystalline cuprates. For misalignment angles between adjacent grains above $\Theta_c \sim 3°$, J_c drops exponentially [32]. Unfortunately, such an exponential decay of the current as a function of the misalignment angle between grains was measured in the FeSCs as well, namely in 122 films grown onto bicrystal substrates. However, the suppression of J_c is not as strong as in high-T_c cuprates; indeed it was found that the critical angle for J_c suppression is slightly larger than in cuprates $\Theta_c \sim 9°$ and the suppression itself is less severe, for example for Θ from 0° to 24° J_c decreases by one order of magnitude in $Ba(Fe_{1-x}Co_x)_2As_2$ and by two orders of magnitude in $YBa_2Cu_3O_{7-x}$ [33, 34]. On the other hand, it was suggested that 'real' grain boundaries can often show much better transparency than the planar grain boundaries of the bicrystals [35], because the misorientation angle is not the only parameter that determines whether or not grain boundaries are transparent to the supercurrent. In addition, the orientation of the field with respect to the grain boundary has to be taken into account, because the inter-grain J_c degrades the most when a significant portion of the vortex lies in the grain boundary. When the vortex obliquely crosses the grain boundary, the suppression of the inter-grain J_c is much weaker.

On the whole, it can be stated that the weak link problem is less serious in FeSCs than in cuprates [36]. The mechanisms that limit current flow at the grain boundaries in FeSCs are still lacking a well-founded explanation. There are likely a number of reasons, both intrinsic and extrinsic, such as the larger critical angle Θ_c, possibly related to the higher robustness of the superconducting s-wave symmetry as compared to d-wave symmetry in cuprates, and the metallic nature of underdoped phases that may be present at the grain boundaries as compared to the insulating nature of cuprate parent compounds.

Magnetic granularity in the cuprates was (at least partly) overcome by texturing in the coated conductor technology. A high degree of texture ensures a small density of high angle grain boundaries that would reduce the macroscopic current. The corresponding production techniques, however, involve multiple steps with related costs.

Texturing might not be necessary for the FeSCs. In particular, results on K-doped 122 wires are encouraging, since current densities that approach the requirements of applications have been demonstrated (see section 3). A combination of the more favorable grain coupling and nano-sized grains enable current densities in granular iron-based materials, which are orders of magnitude higher than the best results achieved in untextured cuprates.

Overdoping has a beneficial effect on the inter-grain transport in cuprates, specifically Ca doping in Y-123 [37]. Analogously, it was found that Sn addition largely improves inter-grain connectivity and thus J_c in $SmFeAs(O_{1-x}F_x)$, which exceeds $1{\cdot}10^4$ A cm^{-2} at 5 K [38]. In addition, inter-grain J_c of $Ba(Fe_{1-x}Co_x)_2As_2$ sintered bulk is enhanced by applying low temperature reaction and Co-overdoping up to $x = 0.12$, resulting in a similarly high inter-grain J_c at 5 K [39].

3. Conductor development

The fabrication of conductors for power applications has been explored since the very beginning of the research activity on FeSCs. The current state-of-the-art is not yet mature enough to address the systematic fabrication of long length specimens, but very encouraging results have been obtained on short samples fabricated both by the powder-in-tube (PIT) method and by processes which replicate the *RE*-123 coated conductor technology. Both cases are reviewed in the following sections.

3.1. Powder-in-tube processed conductors

Wires and tapes of all three main FeSC families have been fabricated so far. The quite isotropic character of J_c with respect to the crystalline direction and better coupling between misaligned grains suggests that texturing may not be as stringent as in cuprates, and conductors in the form of untextured wires may achieve the required performance. The fabrication method is PIT, which starts by packing powders into a metallic tube in a high purity Ar atmosphere and sealing the ends. Either powders of the already reacted superconducting phase (*ex situ* PIT) or powders of precursor phases (*in situ* PIT) are used, however for 122 and 1111 families, the *ex situ* process has been used almost exclusively, as it offers more options for optimizing the powder reaction, even by multiple steps. Indeed, powder preparation is crucial for the final result and involves a proper choice of stoichiometry to compensate for element losses during the whole process, the use of high purity precursors, and ball-milling to obtain a smaller grain size and enhance the packing density [40, 41]. The metal tube forming the sheath is generally made of Ag in the case of 122 and 1111 wires and tapes, while a different situation occurs in the case of *in situ* PIT wires and tapes of the 11 phase, where a Fe sheath is employed, as discussed in the following. Indeed, Ag does not react significantly with the superconducting phase at the optimized temperatures of the final thermal treatments and is thus

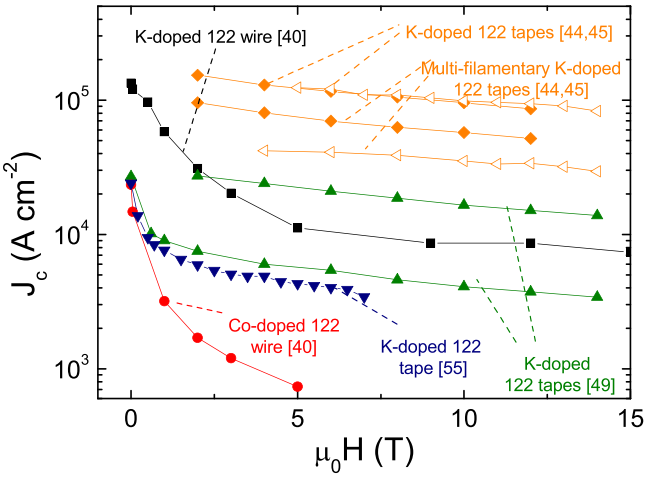

Figure 1. Transport critical current densities at 4.2 K as a function of applied magnetic field. Data refer to K-doped 122 textured tapes with and without chemical additions, prepared by flat rolling and different heat treatments [49, 55], uniaxially mono- and multi-filamentary K-doped 122 tapes prepared using GPa uniaxial pressure [44], mono- and multi-filamentary K-doped 122 tapes prepared using hot pressing at ~30 MPa and 850-900 °C (open symbols) [45], a K-doped 122 untextured wire containing a high density of grain boundaries [40] and a Co-doped untextured wire with a lower density of grain boundaries [40].

preferred over Ta, Nb, Cu and Fe. Ag may be also used in combination with an additional outer sheath made of Fe, Ni or stainless steel [42] to reduce costs and improve the mechanical strength. In this respect, very recently, copper sheathed 122 tapes were fabricated with transport $J_c \sim 3.1{\cdot}10^4$ A cm^{-2} at 10 TT [43], which is noteworthy, given that the use of copper as a sheath material is cost effective, has good mechanical properties and provides reliable thermal stabilization in a magnet during transients. This result was obtained with a hot pressing process where the annealing time was minimized, thus inhibiting the formation of a reaction layer at the copper/superconductor interface. The subsequent step of the PIT process is the deformation, carried out by drawing, groove rolling or flat rolling. Finally, thermal treatments are carried out to form the final phase (*in situ* process) or heal cracks induced by the deformation and enhance grain connectivity and density. The latter goal may be also pursued by performing thermal treatments under high uniaxial pressures. Numberless variations for the deformation and thermal treatment steps are possible and a steady optimization is currently underway.

The best transport critical current values among iron-based superconductor wires and tapes, exceeding 10^5 A cm^{-2}, have been obtained with the 122 family so far [40, 41, 44, 45]. A set of J_c(H) curves measured in 122 wires and tapes, showing the best and most representative behaviors, is presented in figure 1.

Several routes are studied to improve $J_c(H)$ performances. Chemical addition is well-established for improving grain crystallization and enhancing the metallic character of secondary phases at grain boundaries, thus promoting inter-grain coupling. It was shown that 10%–20% Ag substitution

significantly improves inter-grain connectivity and reduces porosity of 122 tapes, resulting in a three times increase of the global J_c up to high fields [46, 47]. Pb addition, on the other hand, promotes grain growth and improves grain connectivity for a content up to 10%, yielding an enhancement of the global J_c in the low field regime [46]. Sn addition has a similar beneficial effect in 122 [48, 49].

Nonetheless, with respect to the role of chemical additions for promoting grain growth, it must be remarked that grain growth is not necessarily the right method to pursue. Indeed, it was shown that untextured polycrystalline $(Ba_{0.6}K_{0.4})Fe_2As_2$ bulks and round wires with high grain boundary density, i.e. small grains obtained by *ex situ* PIT and low temperature (600 °C) thermal treatment, have transport critical current densities well above 10^5 A cm^{-2} in a self-field at 4.2 K [40, 41]. The enhanced grain connectivity was ascribed to significantly improved phase purity. The effectiveness of high density of GBs as pinning centers was explained in terms of low anisotropy and consequent enhanced vortex stiffness of 122 compounds.

Densification of the superconducting core by uniaxial pressing under a high pressure of ∼2 GPa before sintering yielded transport J_c values above 10^5 A cm^{-2}, still as high as $8.6{\cdot}10^4$ A cm^{-2} at 10 T [44]. This result can be attributed to a change in the crack structure and a more uniform deformation achieved by pressing rather than rolling. Indeed, as already observed in Bi-2223 tapes, cracks run transversely to the tape length for rolled tapes and parallel to the tape length for pressed tapes [50]. An optimization of the cold deformation process has to balance the improvement in density and the initiation of microcracks, which cannot be healed by a subsequent heat treatment.

A further improvement in this direction was achieved by a hot pressing technique, which makes the grains more flexible to couple with each other without producing a large number of crashed grains, thus significantly reducing the voids and cracks and leading to a denser superconducting core of PIT tape. More specifically, by pressing K-doped 122 tapes at ∼30 MPa and high temperature T_{HP}, better homogeneity, texture and grain connectivity were obtained, yielding a transport J_c above 10^5 A cm^{-2} at 10 T for $T_{HP} = 850$ °C [45] and even above 10^5 A cm^{-2} at 14 T for $T_{HP} = 900$ °C [51]. However, it should be pointed out that the practical application of uniaxial pressing for the manufacture of long length wires requires specialized machines for continuous pressing of the tape. An easy and simple process is required to balance the high performance and the production cost of the superconducting tapes. So far, through scalable and cheap processes, ∼12 cm long iron-based superconducting tapes with high transport J_c (∼$5.4{\cdot}10^4$ A cm^{-2} [52]–$7.7{\cdot}10^4$ A cm^{-2} [42] at 10 T and 4.2 K) have been obtained. In addition, the fabrication by rolling of a remarkable 11 m long 122 tape, exhibiting fairly uniform J_c throughout the sample, always above $1.5{\cdot}10^4$ A cm^{-2} at 10 T and 4.2 K, has been reported [53]. In scalable processes, mechanical deformation by groove and flat rolling is critical, as its beneficial role in densifying the conductor core and aligning the grains is counterbalanced by the detrimental effect of current blocking transverse cracks generated in the microstructure. Annealing treatments only partially heal microcracks, so that an optimized procedure may require multiple incremental steps of repeated rolling and heat treatment [54].

Improved texture in general improves transport J_c, with values above 10^4 A cm^{-2} [48, 54, 56] up to fields as high as 14 T [49]. Indeed, at high fields, textured tapes perform better than the best untextured wires [49] (figure 1). The beneficial effect of texturing fuelled the idea of preparing iron-based superconductor coated conductors (see section 3.2). Texturing certainly helps to overcome the problems related to anisotropy, but these problems should not be as severe as for high-T_c cuprates, given the smaller values of $J_c^{(ab)}/J_c^{(c)}$ and $B_{c2}^{(ab)}/B_{c2}^{(c)}$ anisotropies found in FeSCs. In addition, the problems related to the current blocking effect resulting from the depressed superconducting order parameter at large angle grain boundaries may have a less important role in FeSCs than in the cuprates. Indeed, as mentioned above, granular iron-based materials exhibit better grain coupling than untextured cuprates, demonstrated by their current densities, which are higher by orders of magnitude than the best results in untextured cuprates. This may be explained also by the clean nature of grain boundaries obtained by an optimized thermal treatment, which drastically reduces Fe_xAs_y secondary phases in the 122 compounds [55].

In fact, a great effort has been carried out with the goal of finding the optimized temperature of thermal treatment T_{tt} to enhance the transport critical current. In general, for tapes, T_{tt} values in the range 700–900 °C are used, while in the case of wires a temperature $T_{tt} = 600$ °C has allowed the best transport $J_c(H = 0)$ values so far [40]. By comparing the preparation conditions of the tapes exhibiting the best self-field and high field transport critical current density, it turns out that with increasing thermal treatment temperature *c*-axis texture, crystallinity and grain connectivity are improved, but eventually secondary Fe_xAs_y phases appear and, in the case of hot uniaxial pressing, transverse microcracks also develop [51]. As a consequence, an optimal T_{tt} can be identified. From the data collection shown in figure 2, it can be gathered that, in terms of maximum self-field transport J_c, such an optimized T_{tt} is 850 °C, regardless of the fabrication either by simple flat rolling or by further application of ∼GPa uniaxial pressure. On the other hand, by assessing the high field $J_c(H \sim 10\ \text{T})$ as a quality parameter, $T_{tt} = 850$ °C is again the best T_{tt} value if the fabrication is carried out with no external applied pressure, while if the process involves application of ∼GPa uniaxial pressure the best $J_c(H \sim 10\ \text{T})$ results are obtained using $T_{tt} = 900$ °C [51]. This difference likely arises from the thermodynamic conditions for secondary phase formation and from the lower volatility of elements under high pressure, which preserves the correct stoichiometry up to higher temperatures. It must be remarked that in some cases, even if no external pressure is applied, the thermal treatment is carried out in sealed stainless steel tubes, which also inhibits the loss of volatile elements [42, 44, 50]. On the other hand, if the thermal treatment is carried out in flowing Ar, following a truly scalable process, the optimal T_{tt} is found to be slightly smaller, namely $T_{tt} = 800$ °C [55]. Note that T_c

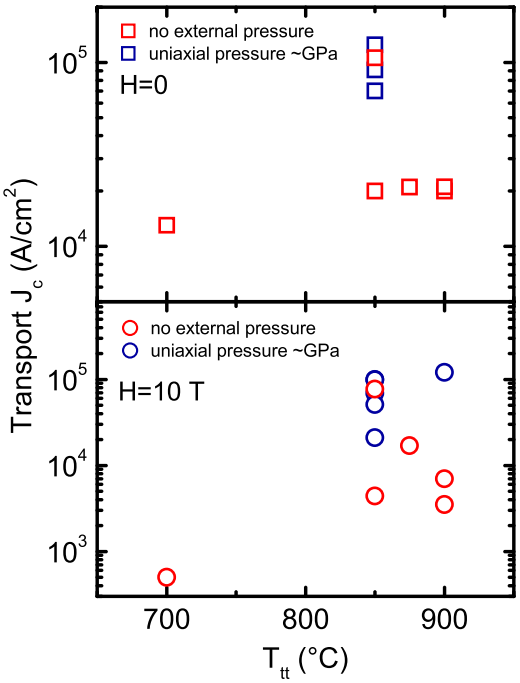

Figure 2. Transport critical current densities of 122 tapes at 4.2 K in zero (upper panel) and 10 T (lower panel) magnetic field plotted as a function of the thermal treatment temperature T_{tt}. Data in zero and high field of samples prepared with no applied external pressure are taken from [42, 49, 50, 56, 78, 84]. Data in zero field of samples prepared at high pressure are taken from [42, 44, 85]. Data at 10T of samples prepared at high pressure are taken from [42, 45, 50, 51, 85].

and J_c are not exactly optimized in the same range of T_{tt} values. The T_c of $Sr_{0.6}K_{0.4}Fe_2As_2$ tapes increases with increasing heat treatment temperature, while maintaining a narrow transition width, up to 900 °C [57]. This behavior is explained by improved crystallinity while approaching the synthesis temperature of precursors, before secondary phases eventually form at $T_{tt} > 900$ °C.

Another key parameter to optimize is the applied pressure, either applied via deformation processes or via isostatic ~GPa uniaxial pressing techniques. Indeed, increasing pressure favors densification and grain connectivity, however it eventually yields to the formation of current blocking microcracks. This parameter does not show a clear tendency in the literature.

As for multi-filamentary 122 iron-pnictide wires and tapes, the highest transport J_c values reached so far are $6.1 \cdot 10^4$ A cm^{-2} and $3.5 \cdot 10^4$ A cm^{-2} at 4.2 K and 10 T, respectively for hot pressed 7- and 19-core Sr-122 tapes [45].

Less work has been carried out for the fabrication of 1111 wires and tapes, due to the difficulty in controlling O and F stoichiometry during heat treatments at high temperatures. The commonly used sintering temperature for 1111 wires is 1200 °C, but sintering at 850 °C–900 °C yielded similarly high-T_c and transport J_c up to 1300 A cm^{-2} [58]. Low temperature sintering allows one to prevent FeAs liquid phases from forming. On the other hand, many unreacted precursors remain in the 1111 bulks even after long sintering, as the reaction rate at low temperatures is relatively small. Moreover, tapes cannot endure long sintering without fluorine loss. In addition, in the case of 1111 wires and tapes, Ag was found to be the best sheath material and metal additions were found to be beneficial. Indeed, the loss of fluorine is reduced and the intergranular coupling enhanced in Sn-added tapes prepared by *ex situ* PIT, exhibiting transport J_c as large as $2.2 \cdot 10^4$ A cm^{-2} at 4.2 K in a self-field [59]. Pre-sintering of Sn-added powders allows one to reduce the FeAs wetting phase and fill the voids between Sm-1111 grains, yielding improved grain connectivity and transport J_c up to $3.45 \cdot 10^4$ A cm^{-2} at 4.2 K in a self-field [60]. However, J_c rapidly decreases with increasing magnetic field, dropping to around 10^2 A cm^{-2} at 8 T [60, 61], possibly as a consequence of the larger anisotropy of the 1111 compounds as compared to the 122 family.

Wires and tapes of the 11 family are appealing for applications as well. Indeed the 11 family, despite its lower T_c, exhibits high J_c and H_{c2} and does not contain toxic elements. Fe(Te,Se) polycrystals prepared by combined melting and annealing processes exhibit a highly homogeneous and dense microstructure, characterized by large and well interconnected grains [62]. A global critical current density, reaching about 10^3 A cm^{-2}, was measured in these samples. Despite this encouraging starting point, several difficulties were encountered in the fabrication of 11 wires and tapes, due to chemical reactions between the superconductor and the sheath during thermal treatments and difficulties in obtaining a high density of powder inside the tube. For this reason, Fe turned out to be the best choice for the sheath, as it allows a diffusion process, where Fe-free precursors are sealed inside Fe tubes and the final 11 phase is formed by the supply of Fe from the sheath during the thermal treatment [63]. This diffusion process yielded a significant improvement in the transport J_c reaching values up to 10^3 A cm^{-2} in FeSe wires [64]. As compared to FeSe, the $FeTe_{0.5}Se_{0.5}$ compound exhibits better superconducting properties in terms of T_c, J_c and H_{c2}. However, only transport J_c values around 220 A cm^{-2} [65] and 400 A cm^{-2} [66] were measured in $FeTe_{0.5}Se_{0.5}$ wires. Indeed, the preparation of Fe(Te,Se) wires and tapes is more difficult [67–69]. It was found that the starting powders de-compose to a Fe_{1+y}(Se,Te) phase with Se/Te ≈ 1 and excess Fe plus a $FeSe_{1-y}$ phase [66] after the heat treatment. The former phase is not superconducting, due to the excess Fe which is detrimental to superconductivity, while the latter phase is superconducting with $T_c \sim 8$ K, much smaller than the $T_c \sim 16$ K of $FeTe_{0.5}Se_{0.5}$. Regarding the optimization of the thermal treatment, it was found that the superconducting properties of FeSe wires improve with increasing annealing temperature up to 1000 °C, where the phase formation is complete [70]. A proper thermal treatment of *ex situ* PIT Fe(Te,Se) wires allows one to enhance the packing density of the core inside the sheath, thanks to the expansion of the lattice volume during the transformation from high density hexagonal $Fe(Te_{0.4}Se_{0.6})_{1.4}$ to low-density tetragonal $FeTe_{0.4}Se_{0.6}$, thus yielding enhanced magnetic J_c up to $3 \cdot 10^3$ A cm^{-2} at 4.2 K in self-field [71].

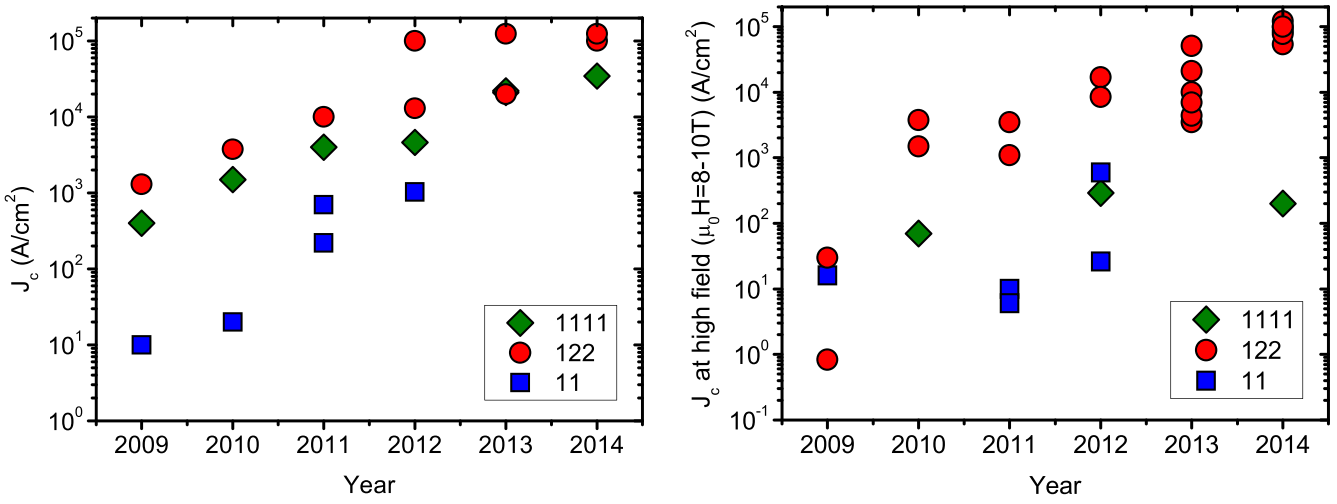

Figure 3. Transport J_c values obtained in iron-based polycrystals, wires and tapes versus the year of publication. In the left panel, data at $T = 4$–5 K and self-field are reported while data at $T = 4$–5 K and a field of 8–10 T are shown in the right panel. References for the left panel are [67] (2009), [20] (2010), [65, 74] (2011), [64] (2012) for the 11 family; [75] (2009), [76] (2010), [48, 77] (2011), [40, 78] (2012), [41, 56] (2013), [42, 44] (2014) for the 122 family; [79] (2009), [58] (2010), [80] (2011), [61] (2012), [59, 81] (2013), [60] (2014) for the 1111 family. for the right panel are [88] (2009), [65, 82] (2011), [62, 64] (2012) for the 11 family; [67] (2009), [83] (2010), [47, 48] (2011), [40, 49] (2012), [41, 50, 54, 56, 84, 85] (2013), [42, 44, 45, 51, 52] (2014) for the 122 family; [58] (2010), [61] (2012), [81] (2013), [60] (2014) for the 1111 family.

In summary, the highest transport critical current in iron-based superconducting wires and tapes have so far been obtained with the 122 family, namely up to 10^4–10^5 A cm^{-2}. Moreover, in 122 wires the J_c field dependence is quite flat, with a decrease of one order of magnitude from a self-field to a field well above 10 T. For the 1111 family, the transport J_c values found in wires and tapes prepared by *ex situ* PIT reach $3.45 \cdot 10^4$ A cm^{-2} [60], but the field dependence of J_c is steeper as compared to 122 wires and tapes [61]. Wires and tapes of the 11 compounds obtained by *in situ* PIT exhibit the lowest transport J_c values, up to $3 \cdot 10^3$ A cm^{-2} [65, 71], but they have the advantages of containing no toxic arsenic and having the simplest crystal structure. The results achieved so far seem to indicate that among the key targets to pursue are (i) improving densification and (ii) inducing a certain degree of texture. Simultaneously, key issues to avoid, not unique to FeSCs, are the segregation of large precipitates at the grain boundaries and the formation of cracks during the deformation process. The best J_c performances are obtained with thermal treatments under high uniaxial pressures, which result in both enhanced density and texture. Hence a finely tuned multi-step protocol of mechanical deformation plus thermal treatment could be set up for tape fabrication, whose effects mimic those of thermal treatments under high uniaxial pressures, minimizing the presence of cracks and fulfilling the further requirement of scalability. However, this would be at the expense of a less favorable geometry, namely tapes instead of wires, the latter being much more favored by engineers. As no evidence of local texture in round conductors, as in the case of melt textured Bi-2212 wires, has ever been detected in FeSCs so far, a possible route could be restacking the tapes into a tube and drawing a wire, similar to the Bi-2212 ROSAT wires [72]. Alternatively, the performances of untextured wires could be improved by grain size refinement, which effectively enhances inter-grain coupling [73].

From the state-of-the art results, it can be envisaged that iron-based superconductor (122) wires and tapes are promising for magnet applications at 20–30 K, where the niobium-based superconductors cannot play a role owing to their lower T_cs, and J_c being rapidly suppressed by the applied field in MgB_2. Moreover, the steady improvements of J_c values achieved in wires and tapes based on 11, 122 and 1111 iron-based superconductors during recent years hardly seem to be saturating yet (figure 3). This positive trend suggests, on one han,d that the inter-grain current in real conductors may behave better than that in epitaxially grown bicrystals, as mentioned above [35]. On the other hand, there exists a considerable potential for future improvements of these materials.

3.2. Coated conductors

As mentioned above, the evidence of weak-linked behavior in 122 thin films grown onto bicrystals suggested the application of the coated conductor technology to iron-based superconductors, i.e. depositing iron-based superconductor films on textured metal substrates with buffer layers, by the techniques successfully developed for second-generation cuprate wires [86, 87]. Ion-beam assisted deposition (IBAD) coated conductor templates are manufactured in two steps. First, an Y_2O_3 layer is made on unpolished Hastelloy by sequential solution deposition to reduce the roughness of the tape surface. Then a biaxially textured MgO layer is deposited on top by IBAD. Through this technique, biaxial texture is achieved by means of a secondary ion gun that orients the oxide film buffer layer while it is being deposited onto the polycrystalline metallic substrate. Alternatively, the RABiTS process for

Table 2. J_c record values of iron-based superconductors coated conductors of different families, measured at low temperature (2.5–5 K) in self-field and high magnetic field, either parallel ($H_{\parallel ab}$) or perpendicular ($H_{\perp ab}$) to the crystalline ab planes (Fe planes).

FeSC family	self-field J_c (A cm^{-2})	in-field $H_{\perp ab}$ J_c (A cm^{-2})	in-field $H_{\parallel ab}$ J_c (A cm^{-2})	Type of measurement	References
122	$3.5 \cdot 10^6$	$1.0 \cdot 10^5$ at $\mu_0 H_{\perp ab} = 10$ T	$2.0 \cdot 10^5$ at $\mu_0 H_{\parallel ab} = 10$ T	transport	[89]
1111	$7 \cdot 10^4$	$5.0 \cdot 10^3$ at $\mu_0 H_{\perp ab} = 4$ T		magnetic	[94]
11	$2.0 \cdot 10^6$	$9.0 \cdot 10^5$ at $\mu_0 H_{\perp ab} = 10$ T	$1.0 \cdot 10^6$ at $\mu_0 H_{\parallel ab} = 10$ T	transport	[9]

coated conductor templates achieves texture by mechanical rolling of a face-centered cubic Ni–W alloy and subsequent heat treatment. A series of biaxially textured buffer oxides, such as Y_2O_3, YSZ and CeO_2 is grown on such metal substrates.

122 films have been grown on IBAD substrates [88–92]. In-plane misorientation of 3°–5° was measured and, most importantly, J_c values of 10^5–10^6 A cm^{-2} were achieved. This route turned out to be encouraging for the 11 family as well. Fe(Se,Te) thin films deposited on IBAD-MgO-buffered Hastelloy substrates were able to carry transport critical current up to $2{\cdot}10^5$ A cm^{-2} at low temperature and self-field, still as high as 10^4 A cm^{-2} at a field of 25 T [93]. Even more remarkable results were obtained for Fe(Se,Te) thin films deposited on RABiTS substrates, namely critical currents up to $2{\cdot}10^6$ A cm^{-2} at low temperature and self-field, still as high as 10^5 A cm^{-2} at a field of 30 T [9]. The fabrication of coated conductors with 1111 FeSCs was also attempted [94]. NdFeAs(O,F) thin films grown by molecular beam epitaxy on IBAD-MgO-Y_2O_3 Hastelloy substrates showed a high *c*-axis texture, but not complete in-plane texture. A magnetic J_c of $7 \cdot 10^4$ A cm^{-2} was measured in a self-field at 5 K , which is larger by one order of magnitude than the J_c of 1111 PIT tapes, but significantly smaller than the J_c of 122 and 11 coated conductors. In addition, the field and temperature dependence of J_c is much stronger than that of coated conductors of the other families, as a consequence of the weak link behavior related to incomplete biaxial texture and the higher anisotropy of this compound. Record data of J_c values measured in coated conductors are reported in table 2.

Remarkably, the challenging fabrication of long (>1 m) coated conductors using a pulsed laser deposition system equipped with a reel-to-reel tape feeding mechanism has already been undertaken [95]. P substituted Ba-122 films were deposited on IBAD-MgO-buffered Hastelloy tapes. J_c measurements on 5 cm and 10 cm pieces yielded $1.1 \cdot 10^5$ A cm^{-2} and $4.7 \cdot 10^4$ A cm^{-2}, respectively. Problems of P loss in the film and inhomogeneity over long lengths were identified.

In the assessment of the potential of coated conductors, it must be pointed out that the thickness of the superconducting layers in coated conductors is currently less than 150 nm. Thicker layers have not been attempted so far but are not expected to be difficult to achieve. Considering the very low engineering critical current density J_e (ratio of critical current I_c to the whole cross-sectional area of conductor), no advantageous points can be found for the iron-based coated conductors compared to the PIT processed tapes and wires at the present stage. Moreover, higher production cost and low production rates of coated conductor technology must be taken into account when assessing the application potential of this process as compared to that of the PIT technology. However, the elaborated oxide buffer structure, partially designed to protect the metal template from oxidation for cuprates wires may not be needed at all for Fe(Se,Te) wires deposited in a vacuum. Growing a Fe(Se,Te) coating directly on textured metal tapes may be possible, thus greatly simplifying the synthesis procedure, reducing production costs and avoiding possible uncontrolled oxygen diffusion into the intermetallic superconductor.

4. Application prospects

From the basic properties discussed above, it could appear that the FeSC can hardly compete with the superior properties of the cuprates. The transition temperature, the upper critical field, and the depairing current density are higher in *RE*-123, on which the coated conductor technology is currently based, than in any iron-based compound. However, the smaller J_d may be balanced by the higher tolerance of the FeSC against a high defect concentration, their smaller anisotropy and the cleaner nature of grain boudaries, all favoring high critical currents at high fields. Thus they may become an alternative for high field conductors at low temperatures.

From an economical point of view, FeSCs have a great potential if the grain coupling can be enhanced further in polycrystalline materials, thus enabling a cheap PIT wire production. Such wires could outperform MgB_2, Nb-Ti and Nb_3Sn conductors at a comparable or even lower price and enable a cost efficient magnet technology operating in the temperature range between 20 K and 30 K, where cryocoolers can be used for cooling instead of liquid helium. If texture is eventually proved to be necessary, the conductors will be more expensive but possibly cheaper than cuprate-based coated conductors, due to the relaxed requirements on texture quality. In addition, a much simpler conductor architecture, with only one buffer layer, has been demonstrated (see subsection 3.2).

The possible operation conditions for applications requiring an engineering current density $J_e > 10^4$ A cm^{-2} are summarized in figure 4. The performance of the FeSC is extrapolated to thick coated conductors or well-connected polycrystalline wires and has not been demonstrated yet. It however shows the potential of the iron-based compounds to replace other materials and to push the current limit of superconducting high field magnets. If the coated conductor technology were necessary for high performance FeSCs – the

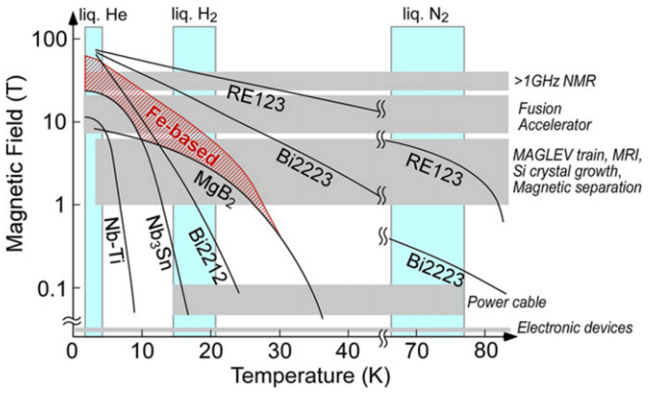

Figure 4. Possible operation conditions for applications requiring $J_e > 10^4$ A cm^{-2} for various superconducting tapes and wires (from [3], copyright 2014 by Institute of Physics). The lines show the limiting fields as a function of temperature.

range of interest (for economic reasons) is marked by the red area – and if PIT wires reached this performance, these conductors would presumably be favorable in the entire region below the red line.

5. Conclusions

The performance of the FeSCs in terms of the highest possible operating temperature as well as achievable fields and currents is between those of the cuprate superconductors and the conventional superconductors (Nb_3Sn, MgB_2 and Nb-Ti); thus they have to be either cheaper than the coated conductors or outperform the conventional wire technology to be of interest for applications. Both scenarios do seem to be realistic. The performance of inexpensive PIT wires and tapes steadily increases and iron-based wires might be applicable at higher temperatures as compared to Nb_3Sn and Nb-Ti or at higher fields as compared to MgB_2. Ultrahigh field magnets on the other hand may be made of iron-based coated conductors, since they could be cheaper than their cuprate counterparts, thanks to a simpler architecture and less stringent texture requirements.

Acknowledgments

This work was supported by the Austrian Science Fund (FWF): P22837-N20 and by the FP7 European project SUPER-IRON (grant agreement No.283204).

References

[1] Kamihara Y, Watanabe T, Hirano M and Hosono H 2008 Iron-based layered superconductor $LaO_{1-x}F_iFeAs$ ($x = 0.05 -0.12$) with $T_c = 26$ K *J. Am. Chem. Soc.* **130** 3296

[2] Putti M *et al* 2010 New Fe-based superconductors: properties relevant for applications *Supercond. Sci. Technol.* **23** 034003

[3] Shimoyama J-I 2014 Potentials of iron-based superconductors for practical future materials *Supercond. Sci. Technol.* **27** 044002

[4] Yakita H *et al* 2014 A new layered iron arsenide superconductor: (Ca,Pr)$FeAs_2$ *J. Am. Chem. Soc.* **136** 846
A S *et al* 2014 Synthesis and physical properties of $Ca_{1-x}RE_xFeAs_2$ with RE = La–Gd *Appl. Phys. Express* **7** 073102

[5] Katrych S *et al* 2014 $L_4Fe_2As_2Te_{1-x}O_{4-y}F_y$ (L = Pr,Sm,Gd): a layered oxypnictide superconductor with T_c up to 45 K *Phys. Rev.* B **89** 024518
Katrych S *et al* 2013 $Pr_4Fe_2As_2Te_{1-x}O_4$: A layered FeAs-based superconductor *Phys. Rev.* **87** 180508(R)

[6] Zhu X, Han F, Mu G, Cheng P, Shen B, Zeng B and Wen H-H 2009 Transition of stoichiometric Sr_2VO_3FeAs to a superconducting state at 37.2 K *Phys. Rev.* B **79** 220512(R)

[7] Pachmayr U, Nitsche F, Luetkens H, Kamusella S, Brückner F, Sarkar R, Klauss H-H and Johrendt D 2015 Coexistence of 3d-Ferromagnetism and Superconductivity in $[(Li_{1-x}Fe_x)OH](Fe_{1-y}Li_y)Se$ *Angew. Chem. Int. Ed.* **54** 293–7

[8] Tarantini C *et al* 2010 Strong vortex pinning in Co-doped $BaFe_2As_2$ single crystal thin films *Appl. Phys. Lett.* **96** 142510

[9] Si W, Han S J, Shi X, Ehrlich S N, Jaroszynski J, Goyal A and Li Q 2013 High current superconductivity in $FeSe_{0.5}Te_{0.5}$-coated conductors at 30 tesla *Nat. Commun.* **4** 1347

[10] Braccini V *et al* 2013 Highly effective and isotropic pinning in epitaxial Fe(Se,Te) thin films grown on CaF2 substrates *Appl. Phys. Lett.* **103** 172601

[11] Kurth F *et al* 2015 Unusually high critical current of clean P-doped $BaFe_2As_2$ single crystalline thin film *Appl. Phys. Lett.* **106** 072602

[12] Iida K *et al* 2013 Oxypnictide SmFeAs(O,F) superconductor: a candidate for high-field magnet applications *Sci. Rep.* **3** 2139

[13] Lee S *et al* 2010 Template engineering of Co-doped $BaFe_2As_2$ single-crystal thin films *Nat. Mater.* **9** 397

[14] Fang L *et al* 2013 Huge critical current density and tailored superconducting anisotropy in $SmFeAsO_{0.8}F_{0.15}$ by low-density columnar-defect incorporation *Nat. Commun.* **4** 2655

[15] Fujioka M *et al* 2013 Phase diagram and superconductivity at 58.1 K in α-FeAs-free $SmFeAsO_{1-x}F_x$ *Supercond. Sci. Technol.* **26** 085023

[16] Liu D *et al* 2012 Electronic origin of high-temperature superconductivity in single-layer FeSe superconductor *Nat. Commun.* **3** 931

[17] Ge J-F, Liu Z-L, Liu C, Gao C-L, Qian D, Xue Q-K, Liu Y and Jia J-F 2014 Superconductivity above 100 K in single-layer FeSe films on doped $SrTiO_3$ *Nat. Mater.* **14** 285

[18] Rotter M, Tegel M and Johrendt D 2008 Superconductivity at 38 K in the Iron Arsenide $(Ba_{1-x}K_x)Fe_2As_2$ *Phys. Rev. Lett.* **101** 107006

[19] Fang M H, Pham H M, Qian B, Liu T J, Vehstedt E K, Liu Y, Spinu L and Mao Z Q 2008 Superconductivity close to magnetic instability in $Fe(Se_{1-x}Te_x)_{0.82}$ *Phys. Rev.* B **78** 224503

[20] Pallecchi I, Tropeano M, Lamura G, Pani M, Palombo M, Palenzona A and Putti M 2012 Upper critical fields and critical current densities of Fe-based superconductors as compared to those of other technical superconductors *Physica* C **482** 68

[21] Jooss C, Warthmann R, Kronmüller H, Haage T, Habermeier H-U and Zegenhagen J 1999 Vortex pinning due to strong quasiparticle scattering at antiphase boundaries in YBa2Cu3$O_{7-\delta}$ *Phys. Rev. Lett.* **82** 632

[22] Godeke A 2005 Performance boundaries in Nb_3Sn superconductors *PhD Thesis* University of Twente, Enschede, The Netherlands ISBN90-365-224-2

[23] Xu S Y, Wertz Q L , E, Hu Y F, Pogrebnyakov A V, Zeng X H, Xi X X and Redwing J M 2003 High critical

current density and vortex pinning of epitaxial MgB_2 thin films *Phys. Rev.* B **68** 224501
[24] Eisterer M, Mishev V, Zehetmayer M, Zhigadlo N D, Katrych S and Karpinski J 2014 Critical current anisotropy in Nd-1111 single crystals and the infuence of neutron irradiation *Supercond. Sci. Technol.* **27** 044009
[25] Bellingeri E *et al* 2012 Strong vortex pinning in $FeSe_{0.5}Te_{0.5}$ epitaxial thin film *Appl. Phys. Lett.* **100** 082601
[26] Nakajima Y, Tsuchiya Y, Taen T, Tamegai T, Okayasu S and Sasase M 2009 Enhancement of critical current density in Co-doped $BaFe_2As_2$ with columnar defects introduced by heavy-ion irradiation *Phys. Rev.* B **80** 012510
[27] Eisterer M, Zehetmayer M, Weber H W, Jiang J, Weiss J D, Yamamoto A and Hellstrom E E 2009 Effects of disorder on the superconducting properties of $BaFe_{1.8}Co_{0.2}As_2$ single crystals *Supercond. Sci. Technol.* **22** 095011
[28] Tarantini C, Lee S, Kametani F, Jiang J, Weiss J D, Jaroszynski J, Folkman C M, Hellstrom E E, Eom C B and Larbalestier D C 2012 Artificial and self-assembled vortex-pinning centers in superconducting $Ba(Fe_{1-x}Co_x)_2As_2$ thin films as a route to obtaining very high critical-current densities *Phys. Rev.* B **86** 214504
[29] Moll P J W, Puzniak R, Balakirev F, Rogacki K, Karpinski J, Zhigadlo N D and Batlogg B 2010 High magnetic-field scales and critical currents in SmFeAs(O, F) crystals *Nat. Mater.* **9** 628
[30] Tanatar M A, Ni N, Martin C, Gordon R T, Kim H, Kogan V G, Samolyuk G D, Bud'ko S L, Canfield P C and Prozorov R 2009 Anisotropy of the iron pnictide superconductor $Ba(Fe_{1-x}Co_x)_2As_2$ ($x = 0.074$, $T_c = 23$ K) *Phys. Rev.* B **79** 094507
[31] Crabtree G W, Liu J Z, Umezawa A, Kwok W K, Sowers C H, Malik S K, Veal B W, Lam D J, Brodsky M B and Downey J W 1987 Large anisotropic critical magnetization currents in single-crystal $YBa_2Cu_3O_{7-\delta}$ *Phys. Rev.* B **36** 4021
[32] Hilgenkamp H and Mannhart J 2002 Grain boundaries in high-T_c superconductors *Rev. Mod. Phys.* **74** 485
[33] Lee S *et al* 2009 Weak-link behavior of grain boundaries in superconducting $Ba(Fe_{1-x}Co_x)_2As_2$ bicrystals *Appl. Phys. Lett.* **95** 212505
[34] Katase T, Ishimaru Y, Tsukamoto A, Hiramatsu H, Kamiya T, Tanabe K and Hosono H 2011 Advantageous grain boundaries in iron pnictide superconductor *Nat. Commun.* **2** 409
[35] Durrell J H, Eom C-B, Gurevich A, Hellstrom E E, Tarantini C, Yamamoto A and Larbalestier D C 2011 The behavior of grain boundaries in the Fe-based superconductor *Rep. Prog. Phys.* **74** 124511
[36] Graser S, Hirschfeld P J, Kopp T, Gutser R, Andersen B M and Mannhart J 2010 How grain boundaries limit supercurrents in high-temperature superconductors *Nat. Mater.* **6** 609
[37] Schmehl A, Goetz B, Schulz R R, Schneider C W, Bielefeld H, Hilgenkamp H and Mannhart J 1999 Doping-induced enhancement of the critical currents of grain boundaries in $YBa_2Cu_3O_{7-\delta}$ *Europhys. Lett.* **47** 110
[38] Singh S J, Shimoyama J-I, Ogino H, Yamamoto A and Kishio K 2014 Enhancement of intergranular current density of Sm-based oxypnictide superconductors with Sn addition *Supercond. Sci. Technol.* **27** 085010
[39] Okada T, Ogino H, Yakita H, Yamamoto A, Kishio K and Shimoyama J 2014 Effects of post-annealing and cobalt co-doping on superconducting properties of $(Ca,Pr)Fe_2As_2$ single crystals *Physica* C **505** 1
[40] Weiss J D, Tarantini C, Jiang J, Kametani F, Polyanskii A A, Larbalestier D C and Hellstrom E E 2012 High intergrain critical current density in fine-grain $(Ba_{0.6}K_{0.4})Fe_2As_2$ wires and bulks *Nat. Mater.* **11** 682
[41] Weiss J D, Jiang J, Polyanskii A A and Hellstrom E E 2013 Mechanochemical synthesis of pnictide compounds and superconducting $Ba_{0.6}K_{0.4}Fe_2As_2$ bulks with high critical current density *Supercond. Sci. Technol.* **26** 074003
[42] Gao Z, Togano K, Matsumoto A and Kumakura H 2015 High transport J_c in magnetic fields up to 28 T of stainless steel/Ag double sheathed Ba122 tapes fabricated by scalable rolling process *Supercond. Sci. Technol.* **28** 012001
[43] Lin H, Yao C, Zhang H, Zhang X, Zhang Q, Dong C, Wang D and Ma Y 2015 Large transport J_c in Cu-sheathed $Sr_{0.6}K_{0.4}Fe_2As_2$ superconducting tape conductors *Sci. Rep.* **5** 11506
[44] Gao Z, Togano K, Matsumoto A and Kumakura H 2014 Achievement of practical level critical current densities in $Ba_{1-x}K_xFe_2As_2$/Ag tapes by conventional cold mechanical deformation *Sci. Rep.* **4** 04065
[45] Zhang X *et al* 2014 Realization of practical level current densities in $Sr_{0.6}K_{0.4}Fe_2As_2$ tape conductors for high-field applications *Appl. Phys. Lett.* **104** 202601
[46] Ma Y, Wang L, Qi Y, Gao Z, Wang D and Zhang X 2011 Development of powder-in-tube processed iron pnictide wires and tapes *IEEE Trans. Appl. Supercond.* **21** 2878
[47] Togano K, Matsumoto A and Kumakura H 2011 Large transport critical current densities of Ag sheathed (Ba,K) Fe_2As_2 + Ag Superconducting wires fabricated by an Ex-situ powder-in-tube process *Appl. Phys. Express* **4** 043101
[48] Gao Z, Wang L, Yao C, Qi Y, Wang C, Zhang X, Wang D, Wang C and Ma Y 2011 High transport critical current densities in textured Fe-sheathed $Sr_{1-x}K_xFe_2As_2$+Sn superconducting tapes *Appl. Phys. Lett.* **99** 242506
[49] Gao Z, Ma Y, Yao C, Zhang X, Wang C, Wang D, Awaji S and Watanabe K 2012 High critical current density and low anisotropy in textured $Sr_{1-x}K_xFe_2As_2$ tapes for high field applications *Sci. Rep.* **2** 998
[50] Togano K, Gao Z, Matsumoto A and Kumakura H 2013 Enhancement in transport critical current density of ex situ PIT Ag/(Ba,K)Fe_2As_2 tapes achieved by applying a combined process of flat rolling and uniaxial pressing *Supercond. Sci. Technol.* **26** 115007
[51] Lin H *et al* 2014 Hot pressing to enhance the transport J_c of $Sr_{0.6}K_{0.4}Fe_2As_2$ superconducting tapes *Sci. Rep.* **4** 6944
[52] Dong C, Yao C, Lin H, Zhang X, Zhang Q, Wang D, Ma Y, Oguro H, Awaji S and Watanabe K 2015 High critical current density in textured Ba-122/Ag tapes fabricated by a scalable rolling process *Scr. Mater.* **99** 33
[53] Ma Y 2015 Development of high-performance iron-based superconducting wires and tapes *Physica* C **516** 17
Zhang X, Lin H, Yao C and Ma Y 2014 *Invited presentation at the 2014 Applied Superconductivity Conference* (August 10-15) (*Charlotte, USA*)
[54] Togano K, Gao Z, Taira H, Ishida S, Kihou K, Iyo A, Eisaki H, Matsumoto A and Kumakura H 2013 Enhanced high-field transport critical current densities observed for ex situ PIT processed Ag/(Ba, K)Fe_2As_2 thin tapes *Supercond. Sci. Technol.* **26** 065003
[55] Malagoli A, Wiesenmayer E, Marchner S, Johrendt D, Genovese A and Putti M 2015 Role of heat and mechanical treatments in the fabrication of superconducting $Ba_{0.6}K_{0.4}Fe_2As_2$ *ex-situ* powder-in-tube tapes *Supercond. Sci. Technol.* **28** 095015
[56] Ma Y, Yao C, Zhang X, Lin H, Wang D, Matsumoto A, Kumakura H, Tsuchiya Y, Sun Y and Tamegai T 2013 Large transport critical currents and magneto-optical imaging of textured $Sr_{1-x}K_xFe_2As_2$ superconducting tapes *Supercond. Sci. Technol.* **26** 035011
[57] Lin H, Yao C, Zhang X, Zhang H, Wang D, Zhang Q and Ma Y 2013 Effects of heating condition and Sn addition on the microstructure and superconducting properties of Sr0.6K0.4Fe2As2 tapes *Physica* C **495** 48

[58] Wang L, Qi Y, Wang D, Gao Z, Zhang X, Zhang Z, Wang C and Ma Y 2010 Low-temperature synthesis of $SmFeAsO_{0.7}F_{0.3}$ wires with high transport critical current density *Supercond. Sci. Technol.* **23** 075005

[59] Wang C *et al* 2013 Large transport J_c in Sn-added $SmFeAsO_{1-x}F_x$ tapes prepared by an ex situ PIT method *Supercond. Sci. Technol.* **26** 075017

[60] Zhang Q *et al* 2014 Enhancement of transport critical current density of $SmFeAsO_{1-x}F_x$ tapes fabricated by an *ex-situ* powder-in-tube method with a Sn-presintering process *Appl. Phys. Lett.* **104** 172601

[61] Wang C, Yao C, Zhang X, Gao Z, Wang D, Wang C, Lin H, Ma Y, Awaji S and Watanabe K 2012 Effect of starting materials on the superconducting properties of $SmFeAsO_{1-x}F_x$ tapes *Supercond. Sci. Technol.* **25** 035013

[62] Palenzona A *et al* 2012 A new approach for improving global critical current density in $Fe(Se_{0.5}Te_{0.5})$ polycrystalline materials *Supercond. Sci. Technol.* **25** 115018

[63] Gao Z, Qi Y, Wang L, Wang D, Zhang X, Yao C and Ma Y 2011 Superconducting properties of FeSe wires and tapes prepared by a gas diffusion technique *Supercond. Sci. Technol.* **24** 065022

[64] Ozaki T, Deguchi K, Mizuguchi Y, Kawasaki Y, Tanaka T, Yamaguchi T, Kumakura H and Takano Y 2012 Fabrication of binary FeSe superconducting wires by novel diffusion process *J. Appl. Phys.* **111** 112620

[65] Ozaki T, Deguchi K, Mizuguchi Y, Kawasaki Y, Tanaka T, Yamaguchi T, Tsuda S, Kumakura H and Takano Y 2011 Transport properties and microstructure of mono- and seven-core wires of $FeSe_{1-x}Te_x$ superconductor produced by the Fe-diffusion powder-in-tube method *Supercond. Sci. Technol.* **24** 105002

[66] Palombo M, Malagoli A, Pani M, Bernini C, Manfrinetti P, Palenzona A and Putti M 2015 Exploring the feasibility of Fe(Se,Te) conductors by *ex-situ* Powder-in-Tube method *J. Appl. Phys.* **117** 213903

[67] Mizuguchi Y, Deguchi K, Tsuda S, Yamaguchi T, Takeya H, Kumakura H and Takano Y 2009 Fabrication of the iron-based superconducting wire using Fe(Se, Te) *Appl. Phys. Express* **2** 083004

[68] Ozaki T, Deguchi K, Mizuguchi Y, Kumakura H and Takano Y 2011 Transport properties of iron-based $FeTe_{0.5}Se_{0.5}$ superconducting wire *IEEE Trans. Appl. Supercond.* **21** 2858

[69] Izawa H, Mizuguchi Y, Fujioka M, Takano Y and Miura O 2014 Fabrication of $FeTe_{0.5}Se_{0.5}$ superconducting wires and tapes by a chemical-transformation PIT process *IEEE Trans. Appl. Supercond.* **24** 6900304

[70] Izawa H, Mizuguchi Y, Ozaki T, Takano Y and Miura O 2012 Evolution of tetragonal phase in the FeSe wire fabricated by a novel chemical-transformation powder-in-tube process *Japan. J. Appl. Phys.* **51** 010101

[71] Izawa H, Mizuguchi Y, Takano Y and Miura O 2014 Fabrication of $FeTe_{0.4}Se_{0.6}$ superconducting tapes by a chemical-transformation PIT process *Physica* C **504** 77

[72] Sato J, Ohata K, Okada M, Tanaka K, Kitaguchi H, Kumakura H, Kiyoshi T, Wada H and Togano K 2001 Two kilometer long Bi-2212 ROSATwires *Physica* C **357-60** 1111

[73] Hecher J, Baumgartner T, Weiss J D, Tarantini C, Yamamoto A, Jiang J, Hellstrom E E, Larbalestier D C and Eisterer M Small grains: a key to high-field applications of granular Ba-122 superconductors? *manuscript to be submitted to Supercond. Sci. Technol.*

[74] Ding Q-P, Mohan S, Tsuchiya Y, Taen T, Nakajima Y and Tamegai T 2011 Low-temperature synthesis of $FeTe_{0.5}Se_{0.5}$ polycrystals with a high transport critical current density *Supercond. Sci. Technol.* **24** 075025

[75] Wang L, Qi Y, Wang D, Zhang X, Gao Z, Zhang Z, Ma Y, Awaji S, Nishijima G and Watanabe K 2010 Large transport critical currents of powder-in-tube $Sr_{0.6}K_{0.4}Fe_2As_2$/Ag superconducting wires and tapes *Physica* C **470** 183

[76] Qi Y, Wang L, Wang D, Zhang Z, Gao Z, Zhang X and Ma Y 2010 Transport critical currents in the iron pnictide superconducting wires prepared by the ex situ PIT method *Supercond. Sci. Technol.* **23** 055009

[77] Togano K, Matsumoto A and Kumakura H 2011 Large transport critical current densities of Ag sheathed (Ba,K) Fe_2As_2+Ag superconducting wires fabricated by an *ex-situ* powder-in-tube process *Appl. Phys. Express* **4** 043101

[78] Ding Q-P, Prombood T, Tsuchiya Y, Nakajima Y and Tamegai T 2012 Superconducting properties and magneto-optical imaging of $Ba_{0.6}K_{0.4}Fe_2As_2$ PIT wires with Ag addition *Supercond. Sci. Technol.* **25** 035019

[79] Kametani F *et al* 2009 Intergrain current flow in a randomly oriented polycrystalline $SmFeAsO_{0.85}$ oxypnictide *Appl. Phys. Lett.* **95** 142502

[80] Fujioka M, Kota T, Matoba M, Ozaki T, Takano Y, Kumakura H and Kamihara Y 2011 Effective *ex-situ* fabrication of F-doped SmFeAsO wire for high transport critical current density *Appl. Phys. Express* **4** 063102

[81] Zhang Q, Wang C, Yao C, Lin H, Zhang X, Wang D, Ma Y, Awaji S and Watanabe K 2013 Combined effect of Sn addition and post-rolling sintering on the superconducting properties of $SmFeAsO_{1-x}F_x$ tapes fabricated by an *ex-situ* powder-in-tube process *J. Appl. Phys.* **113** 123902

[82] Ozaki T, Deguchi K, Mizuguchi Y, Kumakura H and Takano Y 2011 Microstructure and transport properties of $FeTe_{0.5}Se_{0.5}$ superconducting wires fabricated by *ex-situ* Powder-in-tube process *Physica* C **471** 1150

[83] Wang L, Qi Y, Zhang X, Gao Z, Wang D and Ma Y 2010 The role of silver addition on the structural and superconducting properties of polycrystalline $Sr_{0.6}K_{0.4}Fe_2As_2$ *Supercond. Sci. Technol.* **23** 025027

[84] Yao C, Ma Y, Wang C, Zhang X, Wang D, Wang C, Lin H and Zhang Q 2013 Fabrication and transport properties of $Sr_{0.6}K_{0.4}Fe_2As_2$ multifilamentary superconducting wires *Appl. Phys. Lett.* **102** 082602

[85] Lin H, Yao C, Zhang X, Zhang H, Wang D, Zhang Q, Ma Y, Awaji S and Watanabe K 2014 Strongly enhanced current densities in $Sr_{0.6}K_{0.4}Fe_2As_2$+Sn superconducting tapes *Sci. Rep.* **4** 4465

[86] Iijima Y, Tanabe N, Kohno O and Ikeno Y 1992 In-plane aligned $YBa_2Cu_3O_{7-x}$ thin films deposited on polycrystalline metallic substrates *Appl. Phys. Lett.* **60** 769

[87] Goyala A *et al* 1996 Epitaxial superconductors on rolling-assisted biaxially-textured substrates (RABiTS): a route towards high critical current density wire *Appl. Supercond.* **4** 403

[88] Iida K, Haenisch J, Huehne R, Kurth F, Kidszun M, Haindl S, Werner J, Schultz L and Holzapfel B 2009 Strong T_c dependence for strained, epitaxial $Ba(Fe_{1-x}Co_x)_2As_2$ thin films *Appl. Phys. Lett.* **95** 192501

[89] Katase T, Hiramatsu H, Matias V, Sheehan C, Ishimaru Y, Kamiya T, Tanabe K and Hosono H 2011 Biaxially textured cobalt-doped $BaFe_2As_2$ films with high critical current density over 1 MA cm^{-2} on MgO-buffered metal-tape flexible substrates *Appl. Phys. Lett.* **98** 242510

[90] Trommler S, Hänisch J, Matias V, Hühne R, Reich E, Iida K, Haindl S, Schultz L and Holzapfel B 2012 Architecture, microstructure and J_c anisotropy of highly oriented biaxially textured Co-doped $BaFe_2As_2$ on Fe/IBAD-MgO-buffered metal tapes *Supercond. Sci. Technol.* **25** 084019

[91] Iida K *et al* 2011 Epitaxial growth of superconducting $Ba(Fe_{1-x}Co_x)_2As_2$ thin films on technical IBAD-MgO substrates *Appl. Phys. Express* **4** 013103

[92] Trommler S, Hühne R, Hänisch J, Reich E, Iida K, Haindl S, Matias V, Schultz L and Holzapfel B 2012 The influence of the buffer layer architecture on transport properties for $BaFe_{1.8}Co_{0.2}As_2$ films on technical substrates *Appl. Phys. Lett.* **100** 122602

[93] Si W, Zhou J, Jie Q, Dimitrov I, Solovyov V, Johnson P D, Jaroszynski J, Matias V, Sheehan C and Li Q 2011 Iron-chalcogenide $FeSe_{0.5}Te_{0.5}$ coated superconducting tapes for high field applications *Appl. Phys. Lett.* **98** 262509

[94] Iida K *et al* 2014 Highly textured oxypnictide superconducting thin films on metal substrates *Appl. Phys. Lett.* **105** 172602

[95] Miyata S, Ishimaru Y, Adachi S, Shimode T, Murai Y, Chikumoto N, Nakao K and Tanabe K 2013 *Extended abstracts of Int. Workshop on Novel Superconductors and Super Materials* (*Tokyo*) p 101

QUERY FORM

JOURNAL: Superconductor Science and Technology

AUTHOR: I Pallecchi *et al*

TITLE: Application potential of Fe-based superconductors

ARTICLE ID: sust519231

The layout of this article has not yet been finalized. Therefore this proof may contain columns that are not fully balanced/ matched or overlapping text in inline equations; these issues will be resolved once the final corrections have been incorporated.

SQ1
Please be aware that the colour figures in this article will only appear in colour in the online version. If you require colour in the printed journal and have not previously arranged it, please contact the Production Editor now.

We have been provided funding information for this article as below. Please confirm whether this information is correct. European Commission: 283204; Austrian Science Fund (FWF): P22837-N20.

Page 13

Q1
Figure 1 does not appear to have been provided, so the figures have been renumbered. Please check.

Page 1

Q2
Please specify the corresponding author and provide his/her email address.

Page 9

Q3
Please check the details for any journal references that do not have a link as they may contain some incorrect information.

Page 11

Q4
Please provide the page range and volume number in reference [73].

Page 11

Q5
Please provide the year of publication in reference [73].
